JACS
JOURNAL OF THE AMERICAN CHEMICAL SOCIETY
Article
Cite This: J. Am. Chem. Soc. XXXX, XXX, XXX−XXX
pubs.acs.org/JACS

Highly Strained, Radially π-Conjugated Porphyrinylene Nanohoops

Youzhi Xu,[†] Sebastian Gsänger,[‡] Martin B. Minameyer,[§] Inhar Imaz,[∥] Daniel Maspoch,[⊥,∥] Oleksandr Shyshov,[†] Fabian Schwer,[†] Xavi Ribas,[#] Thomas Drewello,[§] Bernd Meyer,*[,‡] and Max von Delius*[,†]

[†]Institute of Organic Chemistry, University of Ulm, Albert-Einstein-Allee 11, 89081 Ulm, Germany
[‡]Interdisciplinary Center for Molecular Materials (ICMM) and Computer-Chemistry-Center (CCC), Friedrich-Alexander University Erlangen-Nürnberg, Nägelsbachstrasse 25, 91052 Erlangen, Germany
[§]Department of Chemistry and Pharmacy, Friedrich-Alexander University Erlangen-Nürnberg, Egerlandstrasse 3, 91058 Erlangen, Germany
[∥]Catalan Institute of Nanoscience and Nanotechnology (ICN2), CSIC and the Barcelona Institute of Science and Technology, Campus UAB, 08193 Bellaterra, Barcelona, Catalonia, Spain
[⊥]ICREA, Pg. Lluís Companys 23, 08010 Barcelona, Spain
[#]Institut de Química Computacional i Catàlisi and Departament de Química, Universitat de Girona, Campus Montilivi, 17003 Girona, Catalonia, Spain

Supporting Information

ABSTRACT: Small π-conjugated nanohoops are difficult to prepare, but offer an excellent platform for studying the interplay between strain and optoelectronic properties, and, increasingly, these shape-persistent macrocycles find uses in host−guest chemistry and self-assembly. We report the synthesis of a new family of radially π-conjugated porphyrinylene/phenylene nanohoops. The strain energy in the smallest nanohoop **[2]CPT** is approximately 54 kcal mol^{-1}, which results in a narrowed HOMO−LUMO gap and a red shift in the visible part of the absorption spectrum. Because of its high degree of preorganization and a diameter of ca. 13 Å, **[2]CPT** was found to accommodate C_{60} with a binding affinity exceeding 10^8 M^{-1} despite the fullerene not fully entering the cavity of the host (X-ray crystallography). Moreover, the π-extended nanohoops **[2]CPTN**, **[3]CPTN**, and **[3]CPTA** (N for 1,4-naphthyl; A for 9,10-anthracenyl) have been prepared using the same strategy, and **[2]CPTN** has been shown to bind C_{70} 5 times more strongly than **[2]CPT**. Our failed synthesis of **[2]CPTA** highlights a limitation of the experimental approach most commonly used to prepare strained nanohoops, because in this particular case the sum of aromatization energies no longer outweighs the buildup of ring strain in the final reaction step (DFT calculations). These results indicate that forcing ring strain onto organic semiconductors is a viable strategy to fundamentally influence both optoelectronic and supramolecular properties.

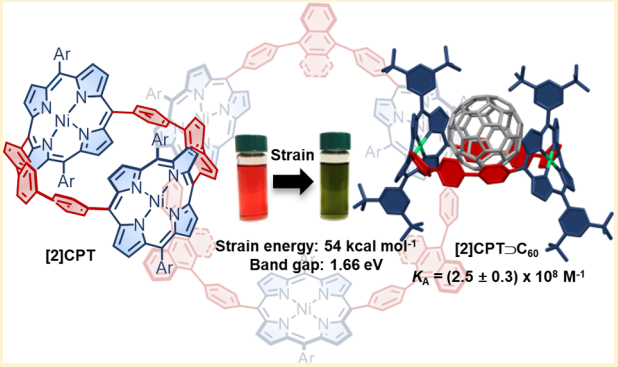

INTRODUCTION

Carbon-rich "nanohoops" exhibiting radial π-conjugation (Figure 1), such as the [*n*]cycloparaphenylenes, have attracted much attention recently due to their challenging synthesis, intriguing optoelectronic properties, and vast potential in supramolecular chemistry.[1] Macrocycles containing porphyrins have been pursued for several decades,[2] leading to important advances in host−guest chemistry[3] and catalysis.[4] Most reported compounds, however, do not exhibit an uninterrupted conjugation pathway or significant ring strain. An exception regarding conjugation is Anderson's work on large porphyrin nanorings,[1b,5] which has produced new concepts of template synthesis[6] and spectacular insights into global (anti)aromaticity[7] as well as charge delocalization.[8] The smallest nanoring synthesized by Anderson features five porphyrin moieties linked by butadiyne spacers that appear to bear most of the moderate ring strain.[9] Osuka's porphyrinelene/phenylene hybrids featuring three to six porphyrins within the macrocycle are subject to significant strain energies (up to 49 kcal mol^{-1}). However, with a diameter of 16 Å, the smallest nanohoop of this series is still too large to effectively accommodate fullerenes.[10]

We wondered whether a smaller variant of Osuka's macrocycles would be accessible based on recent progress in the synthesis of highly strained macrocycles.[11] Specifically, we

Received: August 16, 2019

DOI: 10.1021/jacs.9b08584
J. Am. Chem. Soc. XXXX, XXX, XXX−XXX

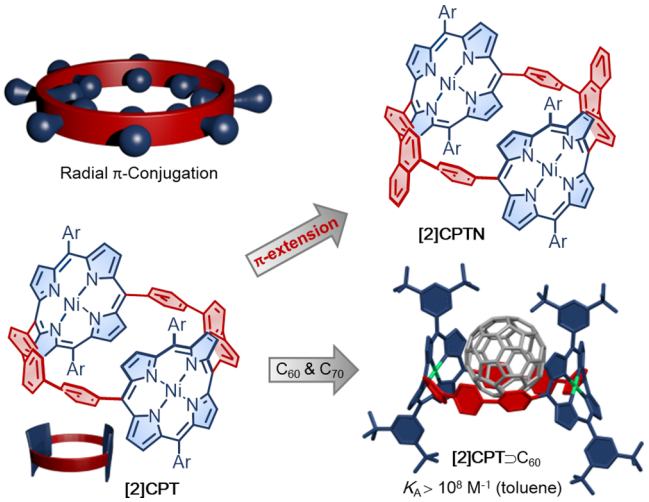

Figure 1. Radially π-conjugated porphyrinylene/phenylene nanohoop.

anticipated that [2]cyclo-5,15-porphyrinylene-4,4′,4″-terphenyl ([**2**]**CPT**) would have a diameter similar to [10]-cycloparaphenylene ([10]CPP), which has recently been shown to be an excellent host for C_{60},[12] enabling studies on noncovalent charge transfer and the synthesis of [2]-rotaxanes.[13,14] Herein, we report that [**2**]**CPT** as highly strained porphyrinylene/phenylene nanohoop can be synthesized in seven linear steps. Although the calculated[15] ring strain of 54 kcal mol^{-1} in this compound is not as high as in the smallest CPP ([5]CPP: 119 kcal mol^{-1}),[16] we observed a strong influence of strain on the absorption, and in contrast to the CPPs the bathochromic shift affects the visible part of the spectrum. We also prepared several π-extended analogues of [*n*]**CPT** and found that members of the [**2**]**CPT** nanohoop family are extremely effective receptors for C_{60} and C_{70} (e.g., Figure 1).

RESULTS AND DISCUSSION

Synthesis of Precursors. The key steps in the synthesis of [*n*]**CPT** are shown in Figure 2a. Diboronate **1** and *meso*-porphyrin **2** are accessible on a multigram scale in four and three linear steps, respectively. Under standard conditions for Suzuki–Miyaura cross-coupling (125 °C, toluene, Cs_2CO_3), we found that the crucial ring-closing step only gave minuscule quantities of the desired small nanohoop [**2**]**CPT-OTES**. In a parameter optimization study for this reaction step, we discovered that the addition of pyridine (100 equiv) led to a significantly increased yield of the desired macrocycle and an unexpected ratio between [**2**]**CPT-OTES** and [**3**]**CPT-OTES** of ca. 2:1. We initially attributed this effect to the binding of pyridine to the nickel center, but, on the basis of the Ni–Ni distance of 7.4 Å in the solid-state structure of [**2**]**CPT-OH** (vide infra) and the highly successful use of pyrazine in preliminary experiments,[17] we believe that a π–π template effect between the electron-deficient heteroarene and the electron-rich porphyrins may be more likely. As shown in Figure 2b, compound [**2**]**CPT-OTES** exhibits a broad peak in the ^{1}H NMR spectrum for the signal corresponding to the *tert*-butyl groups, indicating that the rotation of the *meso*-aryls in [**2**]**CPT-OTES** is relatively slow on the NMR time scale. Variable-temperature (VT) NMR spectroscopy and line-shape analysis allowed us to determine the kinetic parameters (e.g., $\Delta G^{\ddagger}_{298}$ = 14.1 kcal mol^{-1}, Figures S3–S5) for this process,

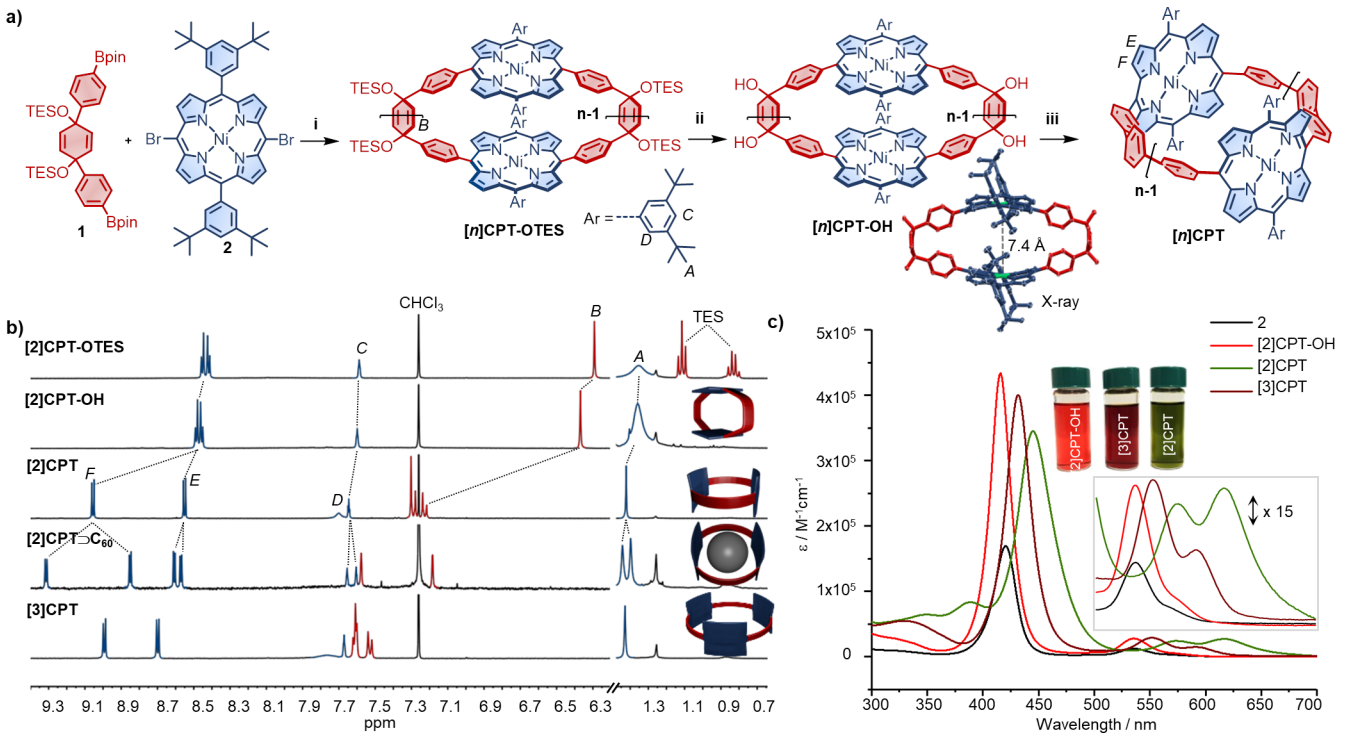

Figure 2. Synthesis of the [*n*]**CPT**. (a) Reaction conditions: (i) $Pd(PPh_3)_4$, Cs_2CO_3, pyridine, toluene, 125 °C, 15 h. (ii) TBAF, THF, rt, 1 h. (iii) H_2SnCl_4, 0 °C → rt, 12 h ([**2**]**CPT** 10%, [**3**]**CPT** 8% three-step yield). (b) Partial ^{1}H NMR spectra ($CDCl_3$, 298 K, 400 MHz): [**2**]**CPT-OTES**, [**2**]**CPT-OH**, [**2**]**CPT**, [**2**]**CPT**⊃C_{60}, and [**3**]**CPT**. (c) UV–vis absorption spectra of **2** (black), [**2**]**CPT-OH** (light red), [**2**]**CPT** (light green), and [**3**]**CPT** (dark red).

DOI: 10.1021/jacs.9b08584
J. Am. Chem. Soc. XXXX, XXX, XXX–XXX

Table 1. Selected Properties of [2]CPT-OH, [3]CPT, [2]CPTN, [3]CPTN, and [3]CPTA

compd	strain energy[a] [kcal mol^{-1}]	λ_{max} (S, Q)[b] [nm]	ε_{max}[b] [L mol^{-1} cm^{-1}]	E^0_{ox1} (E^0_{ox2})[c] [V]	E^0_{red1} (E^0_{red2})[c] [V]	HOMO[d] [eV]	E_g[e] [eV]
[2]CPT-OH	0.8	416, 535, –	4.3×10^5	0.54 (–)	−1.80 (–)	−5.46	2.07
[2]CPT	54.3	446, 575, 617	3.4×10^5	0.32 (0.68)	−1.57 (−1.86)	−5.32	1.66
[3]CPT	34.1	432, 552, 590	4.0×10^5	0.45 (0.84)	−1.77 (−1.98)	−5.43	1.95
[2]CPTN	53.1	442, 567, 610	2.7×10^5	0.34 (0.60)	−1.69 (−1.92)	−5.33	1.78
[3]CPTN		430, 550, 589	4.0×10^5	0.44 (0.73)	−1.79 (−2.04)	−5.44	2.04
[3]CPTA		428, 548, 585	6.2×10^5	0.49 (0.87)	−1.83 (−2.10)	−5.45	2.37

[a]Homodesmotic DFT calculations (B3LYP+D3/def2-TZVP). [b]Measured in CH_2Cl_2. [c]CH_2Cl_2, $TBAPF_6$ (0.1 M), 295 K, V = 100 mV s^{-1}, vs Fc^+/Fc. [d]Set Fc^+/Fc E_{HOMO} = −5.1 eV. [e]Calculated by the difference of the values of E^{onset}_{red1} and E^{onset}_{ox1}.

which we attribute to hindered di(*tert*-butyl)phenyl rotation due to steric clash between the *ortho*-aryl protons and the pyrrole protons.

The isolated compounds [*n*]**CPT-OTES** underwent a smooth transformation into the corresponding alcohols [*n*]**CPT-OH** upon addition of a suitable fluoride reagent. Typically, we converted these intermediates immediately into the target compounds, but in one instance we attempted to purify compound [**2**]**CPT-OH** and were able to grow single crystals suitable for X-ray crystallography. The solid-state structure (Figure 2a) of this compound reveals a rectangular (slightly oval) shape with a Ni−Ni distance of 7.4 Å and two porphyrin macrocycles with a "ruffle" geometry and an offset angle of 80°, which likely helps in avoiding an unfavorable interaction between two *tert*-butyl groups.[18] Because this compound could be of interest as a bimetallic catalyst,[19] it is worth noting that in this solid-state structure the cavity is populated by (masked) solvent molecules and that DFT studies point toward negligible ring strain (Table 1), as well as the ability to adopt a variety of conformations, including some with small cavity volumes (Figure S40).

Nanohoop Synthesis and Characterization. We found that the final aromatization step (Figure 2a) required rigorously optimized reaction conditions, which is presumably a result of the large amount of ring strain generated and the risk of porphyrin degradation.[10] Only when we used the mild reagent H_2SnCl_4[11d] were we able to isolate compounds [**2**]**CPT** and [**3**]**CPT** in reasonable three-step yields of 10% and 6%, respectively. With pure compounds [**2**]**CPT-OH**, [**2**]**CPT**, and [**3**]**CPT** in hand, we proceeded to compare key properties by NMR and UV−vis spectroscopy, cyclic voltammetry, and DFT calculations (Table 1). The ^{1}H NMR spectra (Figure 2b) indicate that, in contrast to the rectangular precursor (vide supra), the rotation of di(*tert*-butyl)phenyl groups is not hindered at room temperature in both [**2**]**CPT** and [**3**]**CPT**, which is likely a consequence of the strain-induced conical arrangement of these groups. Other notable features in the NMR spectra include significant differences in the chemical shifts of aromatic protons (red in Figure 2b) and two sets of signals for pyrrole protons ("*F*" and "*E*"), pointing toward a "ruffle" rather than "saddle" geometry of the porphyrin moieties, which are bent out-of-plane by ca. 35° (C_{meso}−Ni−C_{meso}). A VT-NMR study furthermore revealed that the barrier for the *meso*-aryl C−C bond rotation decreases with increasing nonplanarity of the porphyrin (trend for $\Delta G^{\ddagger}_{298}$: [2]CPT-OTES > [3]CPT > [2]CPT; Figures S4, S9, and S12).

A solid-state structure of [**2**]**CPT** could be obtained by synchrotron X-ray diffraction (Figure 3). Single crystals of [**2**]**CPT** were prepared by slow evaporation of a solution in CH_3CN and $CHCl_3$ (1:1). As shown in Figure 3, [**2**]**CPT** has

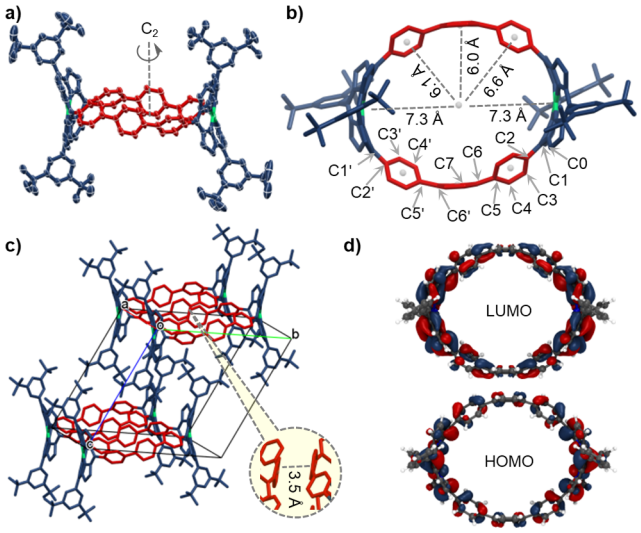

e)

	[2]CPT-OH	[2]CPT
C1-C2	1.49(1) Å	1.45(1) Å
C1'-C2'	1.50(1) Å	1.47(1) Å
C5-C6	1.54(1) Å	1.47(2) Å
C5'-C6'	1.54(1) Å	1.48(2) Å
C0C1C2C3	66°	47°
C4C5C6C7	71°	41°
C7'C6'C5'C4'	19°	35°
C3'C2'C1'C0'	71°	47°

Figure 3. X-ray crystal structure of [**2**]**CPT**: (a) ORTEP drawing with 30% probability. (b) Top view with selected distances and atom numbers. (c) Packing in the unit cell. Hydrogen atoms are omitted for clarity. (d) Frontier molecular orbitals of [**2**]**CPT** calculated at the B3LYP/def2-TZVP level of theory (isovalue 0.018 au). (e) Selected bond lengths and torsional/dihedral (θ) angles in [**2**]**CPT-OH** and [**2**]**CPT**.

an oval shape (approximately C_2 symmetry) with an average diameter of ca. 13.2 Å. The average torsional angle (θ, Figure 3e, bottom) between neighboring phenylene units is 41°, and the phenylene−phenylene bond lengths as well as phenylene−porphyrin bond lengths are shortened by ca. 0.05 Å upon reductive aromatization, suggesting radial conjugation similar to that of the larger [*n*]CPPs.[20]

Furthermore, excessive ring strain seems to be avoided, at least in the solid state, by placing the two face-to-face porphyrins out of a horizontal line. The packing diagram reveals evidence for intermolecular $\pi-\pi$ interactions between the terphenyl bridges (3.5 Å, Figure 3c), which leads to "sideway" stacking of the molecules. In the third dimension, this packing leads to uniform pores with "walls" composed

DOI: 10.1021/jacs.9b08584
J. Am. Chem. Soc. XXXX, XXX, XXX−XXX

nearly exclusively of sp^2-hybridized carbon atoms, which could be of interest for future porous energy storage materials.[21]

Optoelectronic Properties. While the unstrained precursor **[2]CPT-OH** exhibits an absorption spectrum typical for tetraaryl nickel porphyrins (Table 1), we observed significant red shifts for both the Soret (30 nm) and the Q (40 nm) bands for the smallest nanohoop **[2]CPT** when compared to the unstrained reference compound. These red shifts are more pronounced than those found in Osuka's smallest nanohoop[10] (Soret λ_{max} with 435 nm is comparable to **[3]CPT**), which is likely a result of a larger deviation from planarity of the porphyrins. Of note, strain-induced red-shifts are limited to the emission spectra and the ultraviolet part of the spectrum for the related [*n*]CPPs.[1a] Interestingly, there is an inversion in the intensity of the Q bands of the most strained nanohoop **[2]CPT**. Compounds **[3]CPT** and **[2]CPT** were found to be essentially nonfluorescent, which is typical for nickel porphyrins.[22] Data gathered independently by cyclic voltammetry (Figure S26) and DFT calculations (Figures S48–S52, including calculated UV–vis spectra) indicate that the observed bathochromic shifts in the absorption spectrum are due to a narrowing of the HOMO/LUMO gap with increasing ring strain. DFT calculations of the frontier molecular orbitals reveal that for both the HOMO and the LUMO the orbitals are delocalized over the entire ring, yet dominant on the porphyrin moieties (Figure 3d). These results suggest that the incorporation of a dye into a small nanohoop is a viable strategy to exert strain onto the dye and thus change its optoelectronic properties.[23]

Fullerene Complexation. We next turned our attention to the inclusion of fullerene guests into the small nanohoop **[2]CPT**. As shown in Figure 2b, addition of 1 equiv of C_{60} led to dramatic changes in all signal sets of the ^{1}H NMR spectrum as well as a splitting of the pyrrole signals. By means of UV–vis titrations in toluene (Figure 4a; carried out in triplicate), we were able to determine binding constants of ca. 3×10^8 M^{-1} for C_{60} and ca. 2×10^7 M^{-1} for C_{70}. It is worth noting that the strength of fullerene binding is so high that in the MALDI mass spectrum, where noncovalent interactions are typically broken during ionization, the signal for the radical cation of complex **[2]CPT⊃C$_{60}$** is of the same intensity as that for the parent compound **[2]CPT** (Figure 4b). MS/MS experiments revealed that the nanohoop carries the positive charge in the radical cations of the complexes **[2]CPT⊃C$_{60/70}$** (Figures S55 and S56). Collision-induced dissociation experiments at variable collision energies allowed direct comparison of gas-phase relative dissociation energies of fullerene complexes with a monomeric porphyrin (dissociation onset at E_{com} = 0.15 eV), [10]CPP (onset at E_{com} = 0.49 eV), and **[2]CPT**, which in the gas phase binds the larger fullerene C_{70} slightly more strongly than C_{60} (onset at E_{com} = 0.78 and 0.76 eV, respectively).

Single crystals of the **[2]CPT⊃C$_{60}$** complex were grown by slow diffusion of CH_3CN into a mixture of $CHCl_3$ and 1,2-dichlorobenzene (1:1). The solid-state structure clearly shows that a complex between **[2]CPT** and C_{60} with 1:1 stoichiometry is present. As shown in Figure 5a, the encapsulation of C_{60} is clearly facilitated by convex–concave π–π interactions (3.4–3.7 Å) and induces the nanohoop to adopt a more spherical shape. The torsional angle between neighboring phenylene units decreases to 35° (average value), and the ring adopts a conical shape to allow for π–π interactions between terphenyl bridges and C_{60}. According to the solid-state structure, the ^{1}H NMR data, and DFT

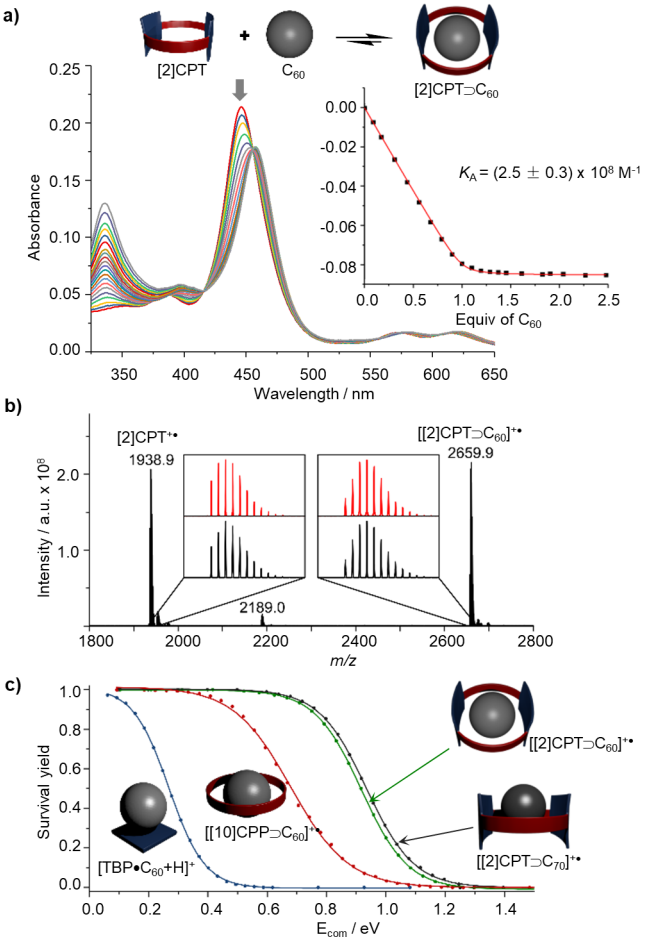

Figure 4. (a) UV–vis titration of **[2]CPT** with C_{60} (0–2.5 equiv) in toluene (fit based on 1:1 model). (b) MALDI mass spectrum of **[2]CPT⊃C$_{60}$** (inset shows the experimental and calculated isotopic pattern). (c) Energy-dependent fragmentation experiments for selected fullerene complexes, each fitted with a sigmoidal Boltzmann function (see Supporting Information, section 8 for details).

calculations (Figure S41), the diameter of **[2]CPT** is slightly too small for a "perfect" (symmetric) encapsulation of C_{60}, which results in "off-center" binding with an offset of 1.9 Å (X-ray). Nevertheless, the calculated deformation energy (upon binding of C_{60}; see Table S12) is less than 1 kcal mol^{-1}, indicating that **[2]CPT** is an outstanding host for C_{60}.

The structure of **[2]CPT⊃C$_{70}$** was studied using DFT calculations, because high-quality single crystals could not be obtained in this particular case. The calculations once more indicate that the fullerene cannot fully enter into the cavity with an offset distance of 2.3 Å, which, as expected, is larger than the corresponding offset for C_{60} (Figure S41). This finding provides an evident opportunity to design related fullerene receptors with even higher binding affinities (vide infra). For both the **[2]CPT⊃C$_{60}$** and the **[2]CPT⊃C$_{70}$** complexes, the HOMO orbital is localized exclusively on porphyrin moieties, while the LUMO orbital is localized dominantly, but not exclusively, on the fullerene (Figures 5d, S53, and S54). Hence, the DFT calculations suggest that charge transfer plays a role in the noncovalent complexes, which is in agreement with the bathochromic shifts observed during the host–guest titrations (Figure 4a).

***π*-Extension of Nanohoops.** Several π-extended CPPs, which can be considered intermediate structures on the way

DOI: 10.1021/jacs.9b08584
J. Am. Chem. Soc. XXXX, XXX, XXX–XXX

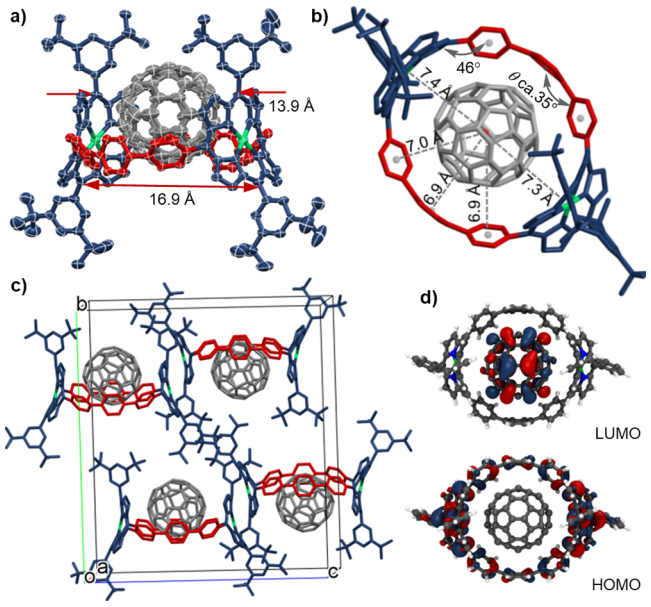

Figure 5. X-ray crystal structure of [2]CPT⊃C_{60}: (a) ORTEP drawing with 30% probability. (b) Top view with distances and dihedral angles labeled. (c) Packing in the unit cell. Hydrogen atoms are omitted for clarity. (d) Frontier molecular orbitals of [2]-CPT⊃C_{60} calculated at the B3LYP/def2-TZVP level of theory (isovalue 0.018 au).

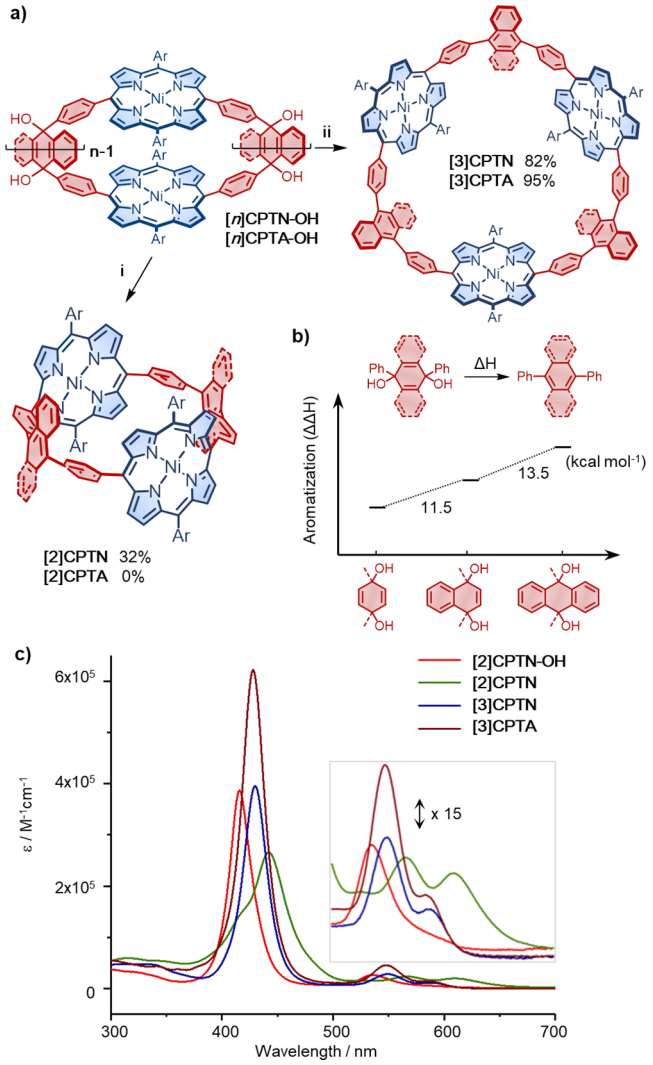

Figure 6. (a) Synthesis of [n]CPTN and [n]CPTA: (i) H_2SnCl_4, rt → 70 °C, THF, 12 h. (ii) H_2SnCl_4, rt, 12 h ([3]CPTN). NaI, NaH_2PO_2, AcOH, 100 °C, 6 h ([3]CPTA). (b) Relative differences in the aromatization enthalpies as calculated at the B3LYP+D3/def2-TZVPP level of theory. (c) UV−vis absorption spectra of [2]CPTN-OH (light red), [2]CPTN (light green), [3]CPTN (blue), and [3]CPTA (dark red).

from CPPs to armchair carbon nanotubes, have been prepared in recent years.[24−26] We wondered whether the inclusion of naphthalene or anthracene moieties would be possible within the [n]CPT architecture. To this end, we start our synthesis from commercially available α-naphthoquinone and anthraquinone to synthesize the diboronate precursors on a multigram scale. Macrocyclic compounds [n]CPTN-OTES and [n]CPTA-OTES (n = 2, 3) were prepared successfully using the same Suzuki−Miyaura cross-coupling conditions with results comparable to those of the parent system. The porphyrin macrocycles could also be transformed smoothly into the corresponding alcohols [n]CPTN-OH and [n]CPTA-OH by treatment with tetrabutylammonium fluoride (TBAF). Strong deviations from the parent system were found in the final step of the synthesis. In case of the naphthyl system, we found that for the small-ring precursor [2]CPTN-OH the final aromatization reaction only proceeded at 70 °C and gave only 32% yield of [2]CPTN after 12 h, whereas the larger [3]CPTN-OH could be easily transformed into [3]CPTN in 82% yield at room temperature (6 h). In case of the anthracenyl system, we failed to convert the small-ring precursor [2]CPTA-OH into [2]CPTA (Figure S24) even at elevated temperature, which indicates that the aromatization energy no longer overcompensates the strain energy. This interpretation is not only in agreement with Clar's "sextet" theory,[27] but was corroborated by DFT calculations, which indeed show that there is a difference of about 20 kcal mol^{-1} (two moieties per ring) in the aromatization enthalpy gain between neighboring compounds in this series (Figure 6b). Hence, by moving from phenyl (reaction efficient at room temperature) to naphthyl (reaction inefficient at elevated temperature) to anthracenyl (reaction impossible), we seem to have probed the limitations of the aromatization versus strain-generation approach that is so commonly used in this field of research.[28] Of note, we can rule out an electronic, and with some confidence also a steric, effect, because the larger precursor [3]CPTA-OH could be converted to [3]CPTA in nearly quantitative yield under mild conditions.

The absorption spectra of the two naphthyl-bridged nanohoops ([2]CPTN and [3]CPTN) are similar to the corresponding [n]CPT nanohoops, but the Soret-band and Q-band absorptions are slightly blue-shifted (Table 1 and Figure 6c). The [3]CPTA absorption maximum was further blue-shifted (428 nm, Table 1), but the most striking observation for this compound is the high molar absorption coefficient of the Soret band ($\varepsilon = 6.2 \times 10^5$ cm^{-1} M^{-1}), which significantly exceeds those determined for all other nanohoops. Differential-pulse voltammetry and cyclic voltammetry experiments of [n]CPTN and [3]CPTA (Figure S26) revealed that these nanohoops exhibit a slightly increased HOMO/LUMO gap when compared to their CPT analogues.[26a]

Depending on the rotation frequency of the phenyl−naphthyl C−C bonds, the π-extended nanohoops of type [n]CPTN can in principle exist as two different stereoisomers,

DOI: 10.1021/jacs.9b08584
J. Am. Chem. Soc. XXXX, XXX, XXX−XXX

which is why we conducted an NMR study to shed light on this issue. The ^{1}H NMR spectra of **[2]CPTN** and **[3]CPTN** showed only one set of signals at room temperature, indicating either fast rotation of the C−C bonds or the presence of only one stereoisomer. Conclusive evidence to this end was obtained by variable-temperature NMR (VT-NMR). The *t*-Bu group signal of **[2]CPT**, **[2]CPTN**, and **[3]CPTN** splits into two peaks at low temperature (ca. 240, 230, and 250 K, respectively), which we attribute to the slow rotation of the porphyrin-((*t*Bu)$_2$-phenyl) C−C bond (see Figures S9, S16, S20, and S21 for VT-NMR spectra and Eyring analyses). Evidence for a restricted rotation of the naphthalene units within the nanohoops was not observed in the investigated temperature range (minimum temperature: 250 K).

To test the limits of fullerene affinity in these new nanohoop architectures, we studied the thermodynamics of **[2]CPTN**⊃fullerene complexes. UV−vis titrations revealed an association constant of 3.0 × 10^8 M^{-1} (toluene) for **[2]CPTN**⊃C_{60} (Figure S32), which is essentially identical to the association constant observed for the **[2]CPT**⊃C_{60} complex. We propose that this unexpected result is due to the cancellation of two effects: π-extension indeed leads to a larger "contact area" and hence stronger association between fullerene and nanohoop, but is offset by a higher energy of deformation, which we determined to be ca. 7 kcal mol^{-1} (DFT; Table S12). When the **[2]CPTN**⊃C_{70} complex was studied in the same way, an increase of the binding constant (1.0 × 10^8 M^{-1}, toluene) by a factor of 5 was observed in comparison to the parent system (Figure 7c). Thanks to the larger VdW surface of C_{70}, in this case the increased interaction between C_{70} and nanohoop outweighs the deformation of the ring (ca. 8 kcal mol^{-1}, DFT, Table S12).

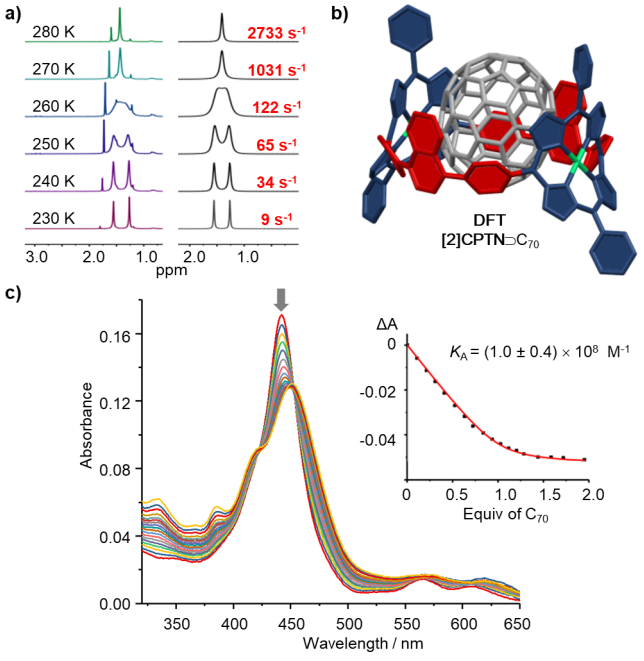

Figure 7. (a) Experimental (left) and simulated (right) ^{1}H NMR spectra of **[3]CPTN** at various temperatures. (b) Optimized geometries of **[2]CPTN**⊃C_{70} obtained by DFT calculations at the PBE+D3 level of theory, with side chains of **[2]CPTN** omitted for clarity. (c) UV−vis titration of **[2]CPTN** with C_{70} (0−1.94 equiv) in toluene (fit based on 1:1 model).

CONCLUSIONS

We developed a concise synthesis of a series of strained porphyrin macrocycles, which due to their unique molecular design offer opportunities for uses in bimetallic catalysis and crystal engineering. The two nanohoops **[2]CPT** and **[2]CPTN** can be considered porphyrinogenic equivalents to [10]CPP, albeit with ca. 100-fold increased affinity for fullerenes, which may prove useful for the regioselective synthesis or separation of fullerene bisadducts[14,29] and in photoelectroactive devices.[30] We also observed unusual optoelectronic properties, most importantly, a strain-induced red-shift of absorption in the visible range of the spectrum, which may inspire further studies on the use of nanohoops for bending organic semiconductors[31] or molecular switches out-of-plane.[32]

ASSOCIATED CONTENT

Supporting Information

The Supporting Information is available free of charge on the ACS Publications website at DOI: 10.1021/jacs.9b08584.

Synthesis and characterization data; details on mass spectrometry, variable-temperature NMR, UV−vis titrations, and theoretical calculations (PDF)
X-ray crystallographic data for **[2]CPT-OH** (CIF)
X-ray crystallographic data for **[2]CPT** (CIF)
X-ray crystallographic data for **[2]CPT**⊃C_{60} (CIF)

AUTHOR INFORMATION

Corresponding Authors

*max.vondelius@uni-ulm.de
*bernd.meyer@fau.de

ORCID

Inhar Imaz: 0000-0002-0278-1141
Daniel Maspoch: 0000-0003-1325-9161
Xavi Ribas: 0000-0002-2850-4409
Bernd Meyer: 0000-0002-3481-8009
Max von Delius: 0000-0003-1852-2969

Notes

The authors declare no competing financial interest.

ACKNOWLEDGMENTS

We are grateful for financial support from the Deutsche Forschungsgemeinschaft (DFG, project number 182849149-SFB953 "Synthetic Carbon Allotropes"), the University of Ulm, and FAU Erlangen-Nürnberg. I.I. thanks the Severo Ochoa Center of Excellence Program (ICN2, Grant SEV-2017-0706), and X.R. is thankful for the ICREA-Acadèmia award.

REFERENCES

(1) (a) Darzi, E. R.; Jasti, R. The Dynamic, Size-Dependent Properties of [5]−[12]Cycloparaphenylenes. *Chem. Soc. Rev.* **2015**, *44*, 6401−6410. (b) Bols, P. S.; Anderson, H. L. Template-Directed Synthesis of Molecular Nanorings and Cages. *Acc. Chem. Res.* **2018**, *51*, 2083−2092. Xu, Y.; von Delius, M. The Supramolecular Chemistry of Strained Carbon Nanohoops. *Angew. Chem., Int. Ed.* **2019**, DOI: 10.1002/anie.201906069.

(2) (a) Aratani, N.; Kim, D.; Osuka, A. Discrete Cyclic Porphyrin Arrays as Artificial Light-Harvesting Antenna. *Acc. Chem. Res.* **2009**, *42*, 1922−1934. (b) Anderson, S.; Anderson, H. L.; Sanders, J. K. M. Expanding Roles for Templates in Synthesis. *Acc. Chem. Res.* **1993**, *11*, 469−475. (c) Jiang, H.; Tanaka, T.; Mori, H.; Park, K. H.; Kim, D.;

DOI: 10.1021/jacs.9b08584
J. Am. Chem. Soc. XXXX, XXX, XXX−XXX

Osuka, A. Cyclic 2,12-Porphyrinylene Nanorings as a Porphyrin Analogue of Cycloparaphenylenes. *J. Am. Chem. Soc.* **2015**, *137*, 2219−2222.
(3) (a) Tashiro, K.; Aida, T. Metalloporphyrin Hosts for Supramolecular Chemistry of Fullerenes. *Chem. Soc. Rev.* **2007**, *36*, 189−197. (b) Yanagisawa, M.; Tashiro, K.; Yamasaki, M.; Aida, T. Hosting Fullerenes by Dynamic Bond Formation with an Iridium Porphyrin Cyclic Dimer: A "Chemical Friction" for Rotary Guest Motions. *J. Am. Chem. Soc.* **2007**, *129*, 11912−11913. (c) Song, J.; Aratani, N.; Shinokubo, H.; Osuka, A. A Porphyrin Nanobarrel That Encapsulates C_{60}. *J. Am. Chem. Soc.* **2010**, *132*, 16356−16357. (d) Kieran, A. L.; Pascu, S. I.; Jarrosson, T.; Sanders, J. K. M. Inclusion of C_{60} into an Adjustable Porphyrin Dimer Generated by Dynamic Disulfide Chemistry. *Chem. Commun.* **2005**, 1276−1278. (e) Tashiro, K.; Hirabayashi, Y.; Aida, T.; Saigo, K.; Fujiwara, K.; Komatsu, K.; Sakamoto, S.; Yamaguchi, K. A Supramolecular Oscillator Composed of Carbon Nanocluster C_{120} and a Rhodium-(III) Porphyrin Cyclic Dimer. *J. Am. Chem. Soc.* **2002**, *124*, 12086−12087. (f) Nobukuni, H.; Shimazaki, Y.; Tani, F.; Naruta, Y. A Nanotube of Cyclic Porphyrin Dimers Connected by Nonclassical Hydrogen Bonds and Its Inclusion of C_{60} in a Linear Arrangement. *Angew. Chem., Int. Ed.* **2007**, *46*, 8975−8978. (g) Xue, S.; Kuzuhara, D.; Aratani, N.; Yamada, H. Synthesis of a Porphyrin(2.1.2.1) Nanobelt and Its Ability to Bind Fullerene. *Org. Lett.* **2019**, *21*, 2069−2072. (h) Gil-Ramírez, G.; Karlen, S. D.; Shundo, A.; Porfyrakis, K.; Ito, Y.; Briggs, G. A. D.; Morton, J. J. L.; Anderson, H. L. A Cyclic Porphyrin Trimer as a Receptor for Fullerenes. *Org. Lett.* **2010**, *12*, 3544−3547.
(4) Walter, C. J.; Anderson, H. L.; Sanders, J. K. M. Q. exo-Selective Acceleration of an Intermolecular Diels−Alder Reaction by a Trimeric Porphyrin Host. *J. Chem. Soc., Chem. Commun.* **1993**, *458*, 458−460.
(5) (a) Hoffmann, M.; Wilson, C. J.; Odell, B.; Anderson, H. L. Template-Directed Synthesis of a π-Conjugated Porphyrin Nanoring. *Angew. Chem., Int. Ed.* **2007**, *46*, 3122−3125. (b) Rickhaus, M.; Vargas Jentzsch, A.; Tejerina, L.; Grübner, I.; Jirasek, M.; Claridge, T. D. W.; Anderson, H. L. Single-Acetylene Linked Porphyrin Nanorings. *J. Am. Chem. Soc.* **2017**, *139*, 16502−16505.
(6) Anderson, H. L.; Sanders, J. K. M. Amine-Template-Directed Synthesis of Cyclic Porphyrin Oligomers. *Angew. Chem., Int. Ed. Engl.* **1990**, *29*, 1400−1403.
(7) Peeks, M. D.; Claridge, T. D. W.; Anderson, H. L. Aromatic and Antiaromatic Ring Currents in a Molecular Nanoring. *Nature* **2017**, *541*, 200−203.
(8) Peeks, M. D.; Tait, C. E.; Neuhaus, P.; Fischer, G. M.; Hoffmann, M.; Haver, R.; Cnossen, A.; Harmer, J. R.; Timmel, C. R.; Anderson, H. L. Electronic Delocalization in the Radical Cations of Porphyrin Oligomer Molecular Wires. *J. Am. Chem. Soc.* **2017**, *139*, 10461−10471.
(9) Liu, P.; Hisamune, Y.; Peeks, M. D.; Odell, B.; Gong, J. Q.; Herz, L. M.; Anderson, H. L. Synthesis of Five-Porphyrin Nanorings by Using Ferrocene and Corannulene Templates. *Angew. Chem., Int. Ed.* **2016**, *55*, 8358−8362.
(10) Jiang, H.; Tanaka, T.; Kim, T.; Sung, Y. M.; Mori, H.; Kim, D.; Osuka, A. Synthesis of [*n*]Cyclo-5,15-porphyrinylene-4,4'-biphenylenes Displaying Size-Dependent Excitation-Energy Hopping. *Angew. Chem., Int. Ed.* **2015**, *54*, 15197−15201.
(11) (a) Jasti, R.; Bhattacharjee, J.; Neaton, J. B.; Bertozzi, C. R. Synthesis, Characterization, and Theory of [9]-, [12]-, and [18]-Cycloparaphenylene: Carbon Nanohoop Structures. *J. Am. Chem. Soc.* **2008**, *130*, 17646−17647. (b) Golder, M. R.; Jasti, R. Syntheses of the Smallest Carbon Nanohoops and the Emergence of Unique Physical Phenomena. *Acc. Chem. Res.* **2015**, *48*, 557−566. (c) Takaba, H.; Omachi, H.; Yamamoto, Y.; Bouffard, J.; Itami, K. Selective Synthesis of [12]Cycloparaphenylene. *Angew. Chem., Int. Ed.* **2009**, *48*, 6112−6116. (d) Patel, V. K.; Kayahara, E.; Yamago, S. Practical Synthesis of [*n*]Cycloparaphenylenes (n = 5, 7−12) by H_2SnCl_4-Mediated Aromatization of 1,4-Dihydroxycyclo-2,5-diene Precursors. *Chem. - Eur. J.* **2015**, *21*, 5742−5749. (e) Iwamoto, T.; Watanabe, Y.; Sakamoto, Y.; Suzuki, T.; Yamago, S. Selective and Random Syntheses of [*n*]Cycloparaphenylenes (n = 8−13) and Size Dependence of Their Electronic Properties. *J. Am. Chem. Soc.* **2011**, *133*, 8354−8361. (f) Lu, D.; Zhuang, G.; Wu, H.; Wang, S.; Yang, S.; Du, P. A Large π-Extended Carbon Nanoring Based on Nanographene Units: Bottom-Up Synthesis, Photophysical Properties, and Selective Complexation with Fullerene C_{70}. *Angew. Chem., Int. Ed.* **2017**, *56*, 158−162. (g) Lu, D.; Cui, S.; Du, P. Large π-Extension of Carbon Nanorings by Incorporating Hexa-peri-hexabenzocoronenes. *Synlett* **2017**, *28*, 1671−1677. (h) Hitosugi, S.; Nakanishi, W.; Yamasaki, T.; Isobe, H. Bottom-up Synthesis of Finite Models of Helical (n, m)-Single-wall Carbon Nanotubes. *Nat. Commun.* **2011**, *2*, 492. (i) Kawase, T.; Darabi, H. R.; Oda, M. Cyclic [6]- and [8]Paraphenylacetylenes. *Angew. Chem., Int. Ed. Engl.* **1996**, *35*, 2664−2666. (j) Lee, S.; Chenard, E.; Gray, D. L.; Moore, J. S. Synthesis of Cycloparaphenyleneacetylene via Alkyne Metathesis: C_{70} Complexation and Copper-Free Triple Click Reaction. *J. Am. Chem. Soc.* **2016**, *138*, 13814−13817. (k) Povie, G.; Segawa, Y.; Nishihara, T.; Miyauchi, Y.; Itami, K. Synthesis of a Carbon Nanobelt. *Science* **2017**, *356*, 172−175. (l) Cheung, K. Y.; Gui, S.; Deng, C.; Liang, H.; Xia, Z.; Liu, Z.; Chi, L.; Miao, Q. Synthesis of Armchair and Chiral Carbon Nanobelts. *Chem.* **2019**, *5*, 838−847. (m) Senthilkumar, K.; Kondratowicz, M.; Lis, T.; Chmielewski, P. J.; Cybińska, J.; Zafra, J. L.; Casado, J.; Vives, T.; Crassous, J.; Favereau, L.; Stępień, M. Lemniscular [16]Cycloparaphenylene: A Radially Conjugated Figure-Eight Aromatic Molecule. *J. Am. Chem. Soc.* **2019**, *141*, 7421−7427. (n) Segawa, Y.; Kuwayama, M.; Hijikata, Y.; Fushimi, M.; Nishihara, T.; Pirillo, J.; Shirasaki, J.; Kubota, N.; Itami, K. Topological Molecular Nanocarbons: All-benzene Catenane and Trefoil Knot. *Science* **2019**, *276*, 272−276.
(12) (a) Iwamoto, T.; Watanabe, Y.; Sadahiro, T.; Haino, T.; Yamago, S. Size-Selective Encapsulation of C_{60} by [10]-Cycloparaphenylene: Formation of the Shortest Fullerene-Peapod. *Angew. Chem., Int. Ed.* **2011**, *50*, 8342−8344. (b) Xia, J.; Bacon, J. W.; Jasti, R. Gram-Scale Synthesis and Crystal Structures of [8]- and [10]CPP, and the Solid-State Structure of C_{60}@[10]CPP. *Chem. Sci.* **2012**, *3*, 3018−3021.
(13) Xu, Y.; Wang, B.; Kaur, R.; Minameyer, M.; Bothe, M.; Drewello, T.; Guldi, D.; von Delius, M. A Supramolecular [10]CPP Junction Enables Efficient Electron Transfer in Modular Porphyrin−[10]CPP⊃Fullerene Complexes. *Angew. Chem., Int. Ed.* **2018**, *57*, 11549−11553.
(14) Xu, Y.; Kaur, R.; Wang, B.; Minameyer, M.; Gsänger, S.; Meyer, B.; Drewello, T.; Guldi, D.; von Delius, M. Concave−Convex $\pi-\pi$ Template Approach Enables the Synthesis of [10]Cycloparaphenylene−Fullerene [2]Rotaxanes. *J. Am. Chem. Soc.* **2018**, *140*, 13413−13420.
(15) To allow adequate comparisons with literature values, we provide calculated strain energies based on the B3LYP functional and a homodesmotic reaction model in this Article. More comprehensive data on ring strain are provided in the Supporting Information, section 7.
(16) (a) Evans, P. J.; Darzi, E. R.; Jasti, R. Efficient Room-Temperature Synthesis of a Highly Strained Carbon Nanohoop Fragment of Buckminsterfullerene. *Nat. Chem.* **2014**, *6*, 404−408. (b) Kayahara, E.; Patel, V. K.; Yamago, S. Synthesis and Characterization of [5]Cycloparaphenylene. *J. Am. Chem. Soc.* **2014**, *136*, 2284−2287.
(17) During the revision stage, we found that the more electron-deficient, hence better π-template pyrazine shifts the selectivity even further toward two-porphyrin macrocycles of **[2]CPT** type. A systematic study of this template effect is ongoing.
(18) In qualitative UV−vis titrations (toluene), we did not observe significant absorption changes when C_{60} was added to rectangular-shaped **[2]CPT-OH**, indicating that the binding of **[2]CPT-OH** to C_{60} is several orders of magnitude weaker than that to **[2]CPT**.
(19) Oldacre, A. N.; Crawley, M. R.; Friedman, A. E.; Cook, T. R. Tuning the Activity of Heterogeneous Cofacial Cobalt Porphyrins for Oxygen Reduction Electrocatalysis through Self-Assembly. *Chem. - Eur. J.* **2018**, *24*, 10984−10987.

DOI: 10.1021/jacs.9b08584
J. Am. Chem. Soc. XXXX, XXX, XXX−XXX

(20) Chen, Hang.; Golder, M. R.; Wang, F.; Jasti, R.; Swan, A. K. Raman Spectroscopy of Carbon Nanohoops. *Carbon* **2014**, *67*, 203−213.
(21) Sakamoto, H.; Fujimori, T.; Li, X.; Kaneko, K.; Kan, K.; Ozaki, N.; Hijikata, Y.; Irle, S.; Itami, K. Cycloparaphenylene as a Molecular Porous Carbon Solid with Uniform Pores Exhibiting Adsorption-Induced Softness. *Chem. Sci.* **2016**, *7*, 4204−4210.
(22) McCarthy, J. R.; Weissleder, R. Model Systems for Fluorescence and Singlet Oxygen Quenching by Metalloporphyrins. *ChemMedChem* **2007**, *2*, 360−365.
(23) (a) Zhylitskaya, H.; Cybińska, J.; Chmielewski, P.; Lis, T.; Stępień, M. Bandgap Engineering in π-Extended Pyrroles. A Modular Approach to Electron-Deficient Chromophores with Multi-Redox Activity. *J. Am. Chem. Soc.* **2016**, *138*, 11390−11398. (b) Haddad, R. E.; Gazeau, S.; Pécaut, J.; Marchon, J. C.; Medforth, C. J.; Shelnutt, J. A. Origin of the Red Shifts in the Optical Absorption Bands of Nonplanar Tetraalkylporphyrins. *J. Am. Chem. Soc.* **2003**, *125*, 1253−1268. (c) Parusel, A. B. J.; Wondimagegn, T.; Ghosh, A. Do Nonplanar Porphyrins Have Red-Shifted Electronic Spectra? A DFT/SCI Study and Reinvestigation of a Recent Proposal. *J. Am. Chem. Soc.* **2000**, *122*, 6371−6374. (d) Evans, J. S.; Musselman, R. L. Red Shifting Due to Nonplanarity in Alkylporphyrins: Solid-State Polarized UV−Vis Spectra and ZINDO Calculations of Two Nickel(II)octaethylporphyrins. *Inorg. Chem.* **2004**, *43*, 5613−5629.
(24) (a) Jia, H.; Gao, Y.; Huang, Q.; Cui, S.; Du, P. Facile Three-Step Synthesis and Photophysical Properties of [8]-, [9]-, and [12]Cyclo-1,4-naphthalene Nanorings via Platinum-Mediated Reductive Elimination. *Chem. Commun.* **2018**, *54*, 988−991. (b) Yagi, A.; Segawa, Y.; Itami, K. Synthesis and Properties of [9]Cyclo-1,4-naphthylene: A π-Extended Carbon Nanoring. *J. Am. Chem. Soc.* **2012**, *134*, 2962−2965.
(25) (a) Huang, Z.; Chen, C.; Yang, X.; Fan, X.; Zhou, W.; Tung, C.; Wu, L.; Cong, H. Synthesis of Oligoparaphenylene-Derived Nanohoops Employing an Anthracene Photodimerization−Cycloreversion Strategy. *J. Am. Chem. Soc.* **2016**, *138*, 11144−11147. (b) Xu, W.; Yang, X.; Fan, X.; W, X.; Tung, C.; Wu, Li.; Cong, H. Synthesis and Characterization of a Pentiptycene-Derived Dual Oligoparaphenylene Nanohoop. *Angew. Chem., Int. Ed.* **2019**, *58*, 3943−3947. (c) Della Sala, P.; Capobianco, A.; Caruso, T.; Talotta, C.; De Rosa, M.; Neri, P.; Peluso, A.; Gaeta, C. An Anthracene-Incorporated [8]Cycloparaphenylene Derivative as an Emitter in Photon Upconversion. *J. Org. Chem.* **2018**, *83*, 220−227.
(26) (a) Iwamoto, T.; Kayahara, E.; Yasuda, N.; Suzuki, T.; Yamago, S. Synthesis, Characterization, and Properties of [4]Cyclo-2,7-pyrenylene: Effects of Cyclic Structure on the Electronic Properties of Pyrene Oligomers. *Angew. Chem., Int. Ed.* **2014**, *53*, 6430−6434. (b) Yagi, A.; Venkataramana, G.; Segawa, Y.; Itami, K. Synthesis and Properties of Cycloparaphenylene-2,7-pyrenylene: a Pyrene-Containing Carbon Nanoring. *Chem. Commun.* **2014**, *50*, 957−959.
(27) Clar, E. *The Aromatic Sextet*; John Wiley & Sons Ltd.: London, 1972.
(28) Lewis, S. E. Cycloparaphenylenes and Related Nanohoops. *Chem. Soc. Rev.* **2015**, *44*, 2221−2304.
(29) (a) Brenner, W.; Ronson, T. K.; Nitschke, J. R. Separation and Selective Formation of Fullerene Adducts within an $M^{II}_8L_6$ Cage. *J. Am. Chem. Soc.* **2017**, *139*, 75−78. (b) Wood, C. S.; Browne, C.; Wood, D. M.; Nitschke, J. R. Fuel-Controlled Reassembly of Metal−Organic Architectures. *ACS Cent. Sci.* **2015**, *1*, 504−509. (c) Fuertes-Espinosa, C.; Gómez-Torres, A.; Morales-Martínez, R.; Rodríguez-Fortea, A.; García-Simón, C.; Gándara, F.; Imaz, I.; Juanhuix, J.; Maspoch, D.; Poblet, J. M.; Echegoyen, L.; Ribas, X. Purification of Uranium-based Endohedral Metallofullerenes (EMFs) by Selective Supramolecular Encapsulation and Release. *Angew. Chem., Int. Ed.* **2018**, *57*, 11294−11299.
(30) Huang, Q.; Zhuang, G.; Jia, H.; Qian, M.; Cui, S.; Yang, S.; Du, P. Photoconductive Curved-Nanographene/Fullerene Supramolecular Heterojunctions. *Angew. Chem., Int. Ed.* **2019**, *58*, 6244−6249.
(31) (a) Zhang, B.; Trinh, M. T.; Fowler, B.; Ball, M.; Xu, Q.; Ng, F.; Steigerwald, L. M.; Zhu, X.; Nuckolls, C.; Zhong, Y. Rigid, Conjugated Macrocycles for High Performance Organic Photodetectors. *J. Am. Chem. Soc.* **2016**, *138*, 16426−16431. (b) Ball, M.; Zhang, B.; Zhong, Y.; Fowler, B.; Xiao, S.; Ng, F.; Steigerwald, M.; Nuckolls, C. Conjugated Macrocycles in Organic Electronics. *Acc. Chem. Res.* **2019**, *52*, 1068−1078.
(32) Bléger, D.; Hecht, S. Visible-Light-Activated Molecular Switches. *Angew. Chem., Int. Ed.* **2015**, *54*, 11338−11349.

DOI: 10.1021/jacs.9b08584
J. Am. Chem. Soc. XXXX, XXX, XXX−XXX